# Elastic Longitudinal Electron Scattering form Factors of $^{9}$Be

R.A. Radhi, N.M.Adeeb and A.K.Hashim
Department of Physics, College of Science, University of Baghdad, Baghdad-Iraq.

**Abstract**

Elastic longitudinal electron scattering form factors have been studied for $^{9}$**Be** $(J^{p}=3/2^{-},T=1/2)$ in the frame work of 1p-shell model, which considered as the core of $^{4}$He With five neucleons disturbuted out of the core. The basis of no-core shell model space with $(0+2)\hbar\omega$ truncations are used also to study the effects of effective charge on the elastic longitudinal form factors. A good agreement of results are obtaining with the experimental data for both models considered in this work. The reduced transition probabilities B(C2) calculated for the two kinds of model space and for the effective charges which are used in this work.

## 1.Introduction

Electron scattering has proven itself as one of the most effective methods of studying the properties of the energy levels of atomic nuclei [1]; so it is a powerful tool to study nuclear structure.

Elastic electron scattering has been mainly employed to measure the charge radius of nuclei and their nuclear surface thickness [2].

Calculations have been performed in the shell model in order to obtain systematic explanation of the lower–lying levels in nuclei, such as $^{9}$**Be** nucleus.

The 1*p*-shell has been a testing ground for nuclear models [3] but inspite of its success in describing the static properties of nuclei it failed to describe electron scattering data without including the core - particle effects [4].These effects are included by giving the model space nucleons effective charges, different from their bare values to account for the discarded space. These effects are called core–polarization effects.

Large–basis no core model calculations have been performed [5,6] for *p*-shell nuclei using six major shells (from 1*s* to 3*p* -2*f* – 1*h* ). In these calculations all nucleons are active. However, constrained by computer capabilities, one can use a truncated no–core calculations, where only those configurations are retained from the full no–core case in which there are up and including few $\hbar\omega$ levels excitations of the lowest unperturbed configuration. As the number of $\hbar\omega$ levels increases, the result will converge and approach those of the full no–core calculations. It was observed [7] that the E2 transition rates obtained in the $4\hbar\omega$ calculations for $^{6}$Li are weaker than those calculated in the $6\hbar\omega$ space. Shell model structure of low – lying excited states in $^{6,7}$Li have been studied [8] using multi-$\hbar\omega$ excitations. However, it was found that the result of the quadrupole moments were far from the experimental values, even with $(0+2+4+6)\hbar\omega$ wave functions. A clear improvement in most observables was evident for the calculation of the $^{10}\mathrm{C}\rightarrow{}^{10}\mathrm{B}$ Fermi matrix elements [9], where the size of the large model space was increased from $2\hbar\omega$ to $4\hbar\omega$. Calculations of E2 transitions and quadrupole moments for A= 7-11 underestimated the data [10] and there were still need for effective charges despite the large model space, $6\hbar\omega$ for A=7 nuclei, and $4\hbar\omega$ for A=8-10 nuclei. Convergent results were obtained for A=3 and A=4 with $5\hbar\omega$ and $16\hbar\omega$, respectively. Radhi et al. [11] have used large basis no core shell model to study the elastic and inelastic electron scattering on $^{19}$F. They found that the results were still far from the experimental values, and excitations out of the no core shell model space are essential in obtaining a reasonable description of longitudinal and transverse electron scattering form factors. In the present work, we will adopt a resitricted *p*- shell model space (model A) and a large no core model space (model B). Excitations out of the model space will be taken into consideration through effective charge model.

## 2.Theory

The reduced one –body matrix element for shell-model wave functions of initial spin $J_i$ and final spin $J_f$ for a given multipolarity $l$

can be expressed as a linear combination of the single - particle matrix elements:

$$\left\langle J_f \left\| \hat{T}_l \right\| J_i \right\rangle = \sum_{J_i J_f} OBDM(j_i, j_f, J_i, J_f, l) \left\langle j_f \left\| \hat{T}_l \right\| j_i \right\rangle \quad \text{.................................} (1)$$

Where the one–body density matrix elements (OBDM) are the structure factors. The initial and final single–particle states are denoted by $j_i$ and $j_f$, respectively.

The reduced single–particle matrix element of the Coulomb (Longitudinal) operator is given by [12]:

$$\left\langle j_f \left\| \hat{T}_l \right\| j_i \right\rangle = \int_0^\infty dr r^2 j_l(qr) \left\langle j_f \left\| Y_l \right\| j_i \right\rangle R_{n_f l_f}(r) R_{n_i l_i}(r) \quad \text{.................................} (2)$$

Where $j_l(qr)$ is the spherical Bessel function and $R_{nl}(r)$ is the single-particle radial wave function.

Electron scattering Coulomb form factor involving angular momentum $l$ and momentum transfer $q$, between initial and final nuclear shell model states of spin $J_{i,f}$ are [12]:

$$\left| F_\lambda(q) \right|^2 = \frac{4\pi}{Z^2(2J_i+1)} \left| \left\langle J_f \left\| \hat{T}_\lambda \right\| J_i \right\rangle \right|^2 \times F_{fs}^2(q) F_{cm}^2(q) \quad \text{.............} (3)$$

Where the nucleon finite size(fs) form factor is $F_{fs}(q) = e^{-(0.43 q^2/4)}$ and $F_{cm}(q) = e^{(q^2 b^2/4A)}$ is the correction for the lack of translation invariance in the shell model (center of mass correction), where $A$ is the mass number and $b$ is the harmonic oscillator size parameter.

The total longitudinal form factor is given by:

$$\left| F(q) \right|^2 = \sum_{l \geq 0} \left| F_l(q) \right|^2 \quad \text{.............................} (4)$$

The electric transition strength is given by:

$$B(C_l, k) = \frac{Z^2}{4p} \left[ \frac{(2l+1)!!}{k^l} \right]^2 F_l^{\,2}(k) \quad \text{......} (5)$$

Where $k = E_x / \mathbf{h}c$, with $E_x$ as the excitation energies.

## 3.Results and Discussion

Calculations of the form factors are presented for the ground state, $J^p T = 3/2^- 1/2$. The measured elastic electron scattering form factors are available from Ref. [13], where the data cover a wide rang of effective momentum transfer.

The radial wave functions for the single-particle matrix elements were calculated with the harmonic oscillator (HO) potential. The oscillator length parameter $b$=1.765$fm$ was chosen to reproduce the measured root mean square charge radius [13].

The 1$p$-shell interaction for both model spaces A and B is represented by the two-body matrix elements [14]. For model space B, the major shells are 1$s$, 1$p$, 2$s$-1$d$, 2$p$-1$f$. We will consider a $(0+2)\mathbf{h}w$ truncation. The $0\mathbf{h}w$ configuration is $[(1s)^4(1p)^5]$, while the $2\mathbf{h}w$ configurations are $[(1s)^3(1p)^5(2s1d)^1]$ and $[(1s)^4(1p)^4(2p1f)^1]$ for one particle – one hole excitation. Also, the $1\mathbf{h}w$ configurations $[(1s)^2(1p)^7]$ and $[(1s)^4(1p)^3(2s1d)^2]$ are allowed for two particle–two hole excitations.

Shell model interactions encompassing the four oscillator shells for this no core model space have been constructed by Warburton and Brown [14]. These interactions are based interactions for the 1$p$2$s$1$d$ shells determined by a least square fit to 216 energy levels in the A=10-22 region assuming no mixing of $n\mathbf{h}w$ and $(0+2)\mathbf{h}w$ configurations. The 1$p$2$s$1$d$ part of the interaction (cited in Ref.[14] as WBP) results from a fit to two–body matrix elements and single–particle energies for the $p$-shell and a potential representation of the 1$p$-2$s$1$d$ cross-shell interaction. The WBP model space was expanded to include 1$s$ and 2$p$1$f$ major shells by adding the appropriate 2$p$1$f$ and cross–shell 2$s$1$d$- 2$p$1$f$ two–body matrix element of the Warburton–Becker–Milliner–Brown (WBMB) interaction [15] and all the necessary matrix elements from the bare G – matrix potential of Hosaka, Kubo and Toki [16]. The 2$s$1$d$ shell interaction of Wildenthal [17] used in WBP interaction is replaced in this study by a new interaction referred as USDB (Universal $sd$-shell B)[18], where the derivation of the USD Hamiltonian [17] has been refined with an up dated and complete set of energy data. The new Hamiltonian USDB leads to a new level of precision for realistic shell–model wave functions.

Shell model calculations were performed with the shell-model code OXBASH[19], where the OBDM elements given in Eq.(1) were obtained.

**3.1. 0.0MeV, $J^{p}=3/2^{-}, T=1/2$ state in 1*p*-shell model space (model space A).**

Elastic longitudinal C0 and C2 form factors calculated with the A model space wave functions are displayed in Figs. (1-3) in comparison with the experimental data of Refs. [13, 20].

C0 and C2 multipolarities of elastic form factor for $^{9}$Be are shown in Fig.(1), which are calculated using bare charge values ($e_p$=1e, $e_n$=0.0) in comparison with the data of Refs.[13,20].

The total C0 + C2 form factor is displayed in Fig. (1b), where the data are slightly underestimated in the region of $q \geq 1.5\, fm^{-1}$.

In addition to the mixing between states contained within the 1*p* shell-model configuration space, mixing with states that lie outside the model space also must be accounted for. Such mixing can be a ccomplished by giving the model space protons and neutrons effective charges different from those of the bare values. Effective charges values of $e_p$=1.35e and $e_n$=0.35e were used by Brown et al.[21] to describe the C2 form factors in *sd* – shell nuclei. We will use these values of effective charges to describe the C2 elastic scattering from $^{9}$Be. Also, values of $e_p$=1.15e and $e_n$=0.45e were used by Glickman et al. [13] to describe C2 elastic and inelastic form factors of $^{9}$Be. Fig. 2 and Fig. 3 show the form factors calculated with $e_p$=1.35e, $e_n$=0.35e and $e_p$=1.15e, $e_n$=0.45e, respectively. The C2 form factors were enhanced from those of the bare charges and described the data very well for all momentum transfer regions, as shown in Fig.(2 b) and Fig. (3 b).

The reduced transition probabilites B(C2) calculated for three values of effective charges are shown in Table (1) in comparison with the measured experimental value 17.1 $e^2.fm^4$ and the theoretical value 9.43 $e^2.fm^4$ of Ref.[13].

***Table (1)***
***The values of the reduced transition probabilities B(C2) (in units of $e^2.fm^4$) using different values of effective charges for the elastic longitudinal transition to the $3/2^{-}\,1/2$ state in $^{9}$Be, using model space A.***

| $e_p$ | $e_n$ | $B(C2)e^2.fm^4$ |
|---|---|---|
| 1e | 0.0 | 5.24 |
| 1.35e | 0.35e | 13.12 |
| 1.15e | 0.45e | 11.0 |

The one-body density matrix elments (OBDM) for protons and neutrons are given in Table (2).

***Table (2)***
***The values of the proton one-body density matrix (OBDMP) and neutron one-body density matrix (OBDMN) elements for the C0 and C2 elastic longitudinal transition to the $3/2^{-}\,1/2$ (0.0MeV)state in $^{9}$Be, using model space A.***

| ***Be$^9$*** | | ***C0*** | |
|---|---|---|---|
| *nlj* | *n′l′j′* | OBDMP | OBDMN |
| $1p_{3/2}$ | $1p_{3/2}$ | –1.61424 | –2.61029 |
| $1p_{1/2}$ | $1p_{1/2}$ | –0.54554 | –0.55119 |
| $1s_{1/2}$ | $1s_{1/2}$ | –2.8284 | –2.8284 |
| ***$^{9}$Be*** | | ***C2*** | |
| *nlj* | *n′l′j′* | OBDMP | OBDMN |
| $1p_{3/2}$ | $1p_{3/2}$ | 0.45586 | 0.31537 |
| $1p_{3/2}$ | $1p_{1/2}$ | 0.29419 | 0.18887 |
| $1p_{1/2}$ | $1p_{3/2}$ | –0.29419 | –0.18887 |

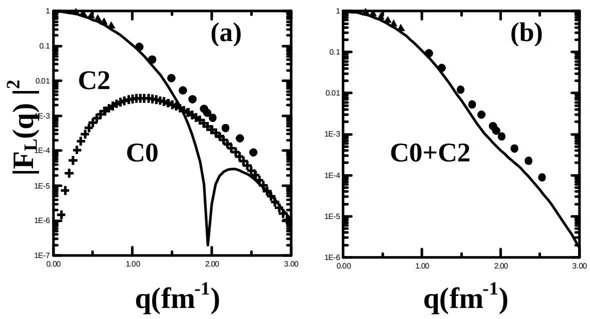


*Fig.(1) Elastic Coulomb form factors calculated with the 1p-shell model space for the transition to the $(3/2^-,1/2)$ (0.0 MeV) state in $^9$Be using ($e_p$=1e, $e_n$=0.0 ). The left panel (a) represents the C0 and C2 longitudinal components. The right panel (b) represents the total longitudinal C0+C2 form factor. The data are taken from Ref.[13] (circles) and Ref. [20] (triangles).*

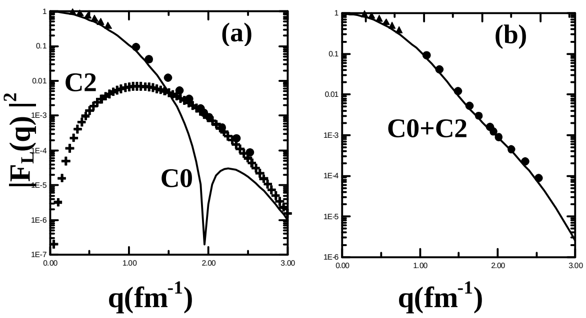


*Fig.(2) Same as caption to Fig.(1), but using $e_p$=1.35e and $e_n$=0.35e effective charges. The data are taken from Ref.[13] (circles) and Ref. [20] (triangles).*

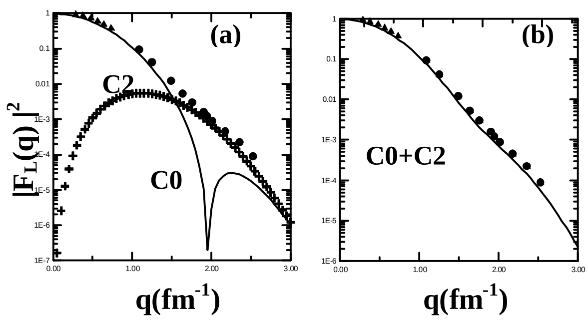


*Fig.(3) Same as caption to Fig.(1), but using $e_p$=1.15e and $e_n$=0.45e effective charges .The data are taken from Ref.[13] (circles) and Ref. [20] (triangles).*

### 3.2 0.0 MeV, $J^p = 3/2^-, T = 1/2$ state no-core model space (model space B).

The calculated C0 and C2 form factors using this model space are shown in Fig. (4 a) and the total C0 + C2 form factor is shown in Fig. (4b), in comparison with the experimental data. As in model space A, the total form factor underestimates the data for $q \geq 1.5\, fm^{-1}$. Extending the model space to include core orbits and orbits outside the 1*p*-shell orbits, with $(0+2)\hbar w$ truncation, dose not modify the form factor from that calculated with the 1*p*–model space alone. Since complete mixing with states that lie outside the model space, can not be performed due to limited computer capabilities. So, we need to go beyond $(0+2)\hbar w$ truncation, which also faced computer capabilities. An alternative is either using a microscopic theory with one particle-one hole excitations, or using effective charges to compensate for the discarded space. As in model space A, we will use same effective charges as those used in model space A. The results are shown in Fig.(5) and Fig.(6), for $e_p$=1.35e, $e_n$=0.35e and $e_p$=1.15e, $e_n$=0.45e, respectively. The data in these cases are very well explained, as shown in Fig. (5 b) and Fig.(6 b).

The calculated B(C2) values are given in Table (3), using different values of effective charges. The measured B(C2) value is 17.1e$^2$.fm$^4$ and theoretical value is 9.43 e$^2$.fm$^4$ [13].

***Table (3)***
***The values of the reduced transition probabilities B(C2) in unit $e^2.fm^4$ using different values of effective charges for the elastic longitudinal transition to the $3/2^-\ 1/2$ state in $^9$Be, using model space B.***

| $e_p$ | $e_n$ | B(C2) $e^2.fm^4$ |
|---|---|---|
| 1e | 0.0 | 4.19 |
| 1.35e | 0.35e | 8.84 |
| 1.15e | 0.45e | 6.88 |

The one-body density matrix elements (OBDM) for protons and neutrons are given in the Tables (4 and 5).

***Table(4)***
***The values of the OBDMP and OBDMN elements for the C0 elastic longitudinal transition to the $3/2^- 1/2$ (0.0MeV) state in $^9Be$, using model space B.***

| $^9Be$ | | C0 | |
|---|---|---|---|
| $nlj$ | $n'l'j'$ | OPDMP | OPDMN |
| $1s_{1/2}$ | $1s_{1/2}$ | –2.76888 | –2.77756 |
| $1s_{1/2}$ | $2s_{1/2}$ | –0.07318 | –0.05496 |
| $1p_{3/2}$ | $1p_{3/2}$ | –1.41034 | –2.39131 |
| $1p_{3/2}$ | $2p_{3/2}$ | –0.05061 | –0.01001 |
| $1p_{1/2}$ | $1p_{1/2}$ | –0.80661 | –0.81536 |
| $1p_{1/2}$ | $2p_{1/2}$ | –0.03453 | –0.03118 |
| $1d_{5/2}$ | $1d_{5/2}$ | –0.02265 | –0.02490 |
| $1d_{3/2}$ | $1d_{3/2}$ | –0.02105 | –0.02169 |
| $2s_{1/2}$ | $1s_{1/2}$ | –0.07318 | –0.05496 |
| $2s_{1/2}$ | $2s_{1/2}$ | –0.01188 | –0.01279 |
| $1f_{7/2}$ | $1f_{7/2}$ | –0.00033 | –0.00051 |
| $1f_{5/2}$ | $1f_{5/2}$ | –0.00033 | –0.00039 |
| $2p_{3/2}$ | $1p_{3/2}$ | –0.05061 | –0.01001 |
| $2p_{3/2}$ | $2p_{3/2}$ | –0.00211 | –0.00450 |
| $2p_{1/2}$ | $1p_{1/2}$ | –0.03453 | –0.03118 |
| $2p_{1/2}$ | $2p_{1/2}$ | –0.00168 | –0.00159 |

***Table(5)***
***The values of the OBDMP and OBDMN elements for the C2 elastic longitudinal transition to $3/2^- 1/2$ (0.0MeV) state in $^9Be$, using model space B.***

| $^9Be$ | | C2 | |
|---|---|---|---|
| $nlj$ | $n'l'j'$ | OBDMP | OBDMN |
| $1s_{1/2}$ | $1d_{5/2}$ | –0.00313 | –0.00427 |
| $1s_{1/2}$ | $1d_{3/2}$ | –0.00397 | –0.00242 |
| $1p_{3/2}$ | $1p_{3/2}$ | 0.33990 | 0.04942 |
| $1p_{3/2}$ | $1p_{1/2}$ | 0.30377 | 0.14905 |
| $1p_{3/2}$ | $1f_{7/2}$ | 0.00106 | 0.00399 |
| $1p_{3/2}$ | $1f_{5/2}$ | –0.00038 | 0.00166 |
| $1p_{3/2}$ | $2p_{3/2}$ | 0.01037 | 0.04879 |
| $1p_{3/2}$ | $2p_{1/2}$ | 0.01170 | 0.00963 |
| $1p_{1/2}$ | $1p_{3/2}$ | –0.30377 | –0.14905 |
| $1p_{1/2}$ | $1f_{5/2}$ | 0.00131 | 0.00091 |
| $1p_{1/2}$ | $2p_{3/2}$ | –0.00892 | –0.00781 |
| $1d_{5/2}$ | $1s_{1/2}$ | –0.00313 | –0.00427 |
| $1d_{5/2}$ | $1d_{5/2}$ | 0.00286 | 0.00204 |
| $1d_{5/2}$ | $1d_{3/2}$ | 0.00197 | 0.00241 |
| $1d_{5/2}$ | $2s_{1/2}$ | 0.00094 | 0.00149 |
| $1d_{3/2}$ | $1s_{1/2}$ | 0.00397 | 0.00242 |
| $1d_{3/2}$ | $1d_{5/2}$ | –0.00197 | –0.00241 |
| $1d_{3/2}$ | $1d_{3/2}$ | 0.00227 | 0.00309 |
| $1d_{3/2}$ | $2s_{1/2}$ | –0.00127 | –0.00106 |
| $2s_{1/2}$ | $1d_{5/2}$ | 0.00094 | 0.00149 |
| $2s_{1/2}$ | $1d_{3/2}$ | 0.00127 | 0.00106 |
| $1f_{7/2}$ | $1p_{3/2}$ | 0.00106 | 0.00399 |
| $1f_{7/2}$ | $1f_{7/2}$ | 0.00005 | 0.00002 |
| $1f_{7/2}$ | $1f_{5/2}$ | 0.00001 | 0.00003 |
| $1f_{7/2}$ | $2p_{3/2}$ | 0.00007 | 0.00005 |
| $1f_{5/2}$ | $1p_{3/2}$ | 0.00038 | –0.00166 |
| $1f_{5/2}$ | $1p_{1/2}$ | 0.00131 | 0.00091 |
| $1f_{5/2}$ | $1f_{7/2}$ | –0.00001 | –0.00003 |
| $1f_{5/2}$ | $1f_{5/2}$ | 0.00005 | 0.00005 |
| $1f_{5/2}$ | $2p_{3/2}$ | 0.00000 | -0.00005 |
| $1f_{5/2}$ | $2p_{1/2}$ | 0.00008 | 0.00003 |
| $2p_{3/2}$ | $1p_{3/2}$ | 0.01037 | 0.04879 |
| $2p_{3/2}$ | $1p_{1/2}$ | 0.00892 | 0.00781 |
| $2p_{3/2}$ | $1f_{7/2}$ | 0.00007 | 0.00005 |
| $2p_{3/2}$ | $1f_{5/2}$ | 0.00000 | 0.00005 |
| $2p_{3/2}$ | $2p_{3/2}$ | 0.00034 | –0.00198 |
| $2p_{3/2}$ | $2p_{1/2}$ | 0.00033 | 0.00034 |
| $2p_{1/2}$ | $1p_{3/2}$ | –0.01170 | –0.00963 |
| $2p_{1/2}$ | $1f_{5/2}$ | 0.00008 | 0.00003 |
| $2p_{1/2}$ | $2p_{3/2}$ | –0.00033 | –0.00034 |

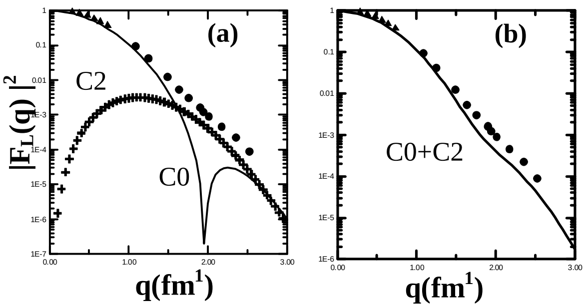


***Fig.(4) Elastic form factors calculated with the spsdpf truncated*** $(0+2)\hbar\omega$ ***no core model space for the transition to the*** $3/2^{-}\ 1/2$ ***(0.0 MeV) state in*** $^{9}$***Be by using*** $e_p$***=1e and*** $e_n$***=0.0, effective charges.The left panel (a) represents the C0 and C2 longitudinal components. The right panel (b) represents the total longitudinal C2+C0. The data are taken from Ref.[13] (circles) and Ref. [20] (triangles).***

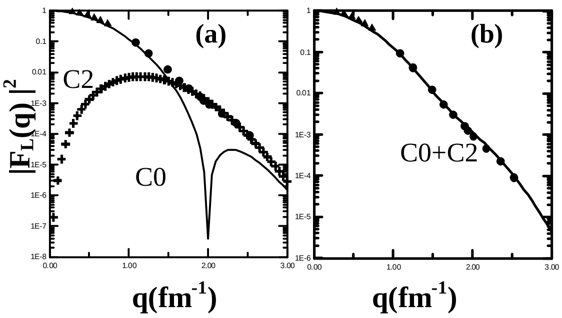


***Fig.(5) Same as caption to Fig.(4), but using*** $e_p$***=1.35e and*** $e_n$***=0.35e effective charges. The data are taken from Ref.[13] (circles) and Ref. [20] (triangles).***

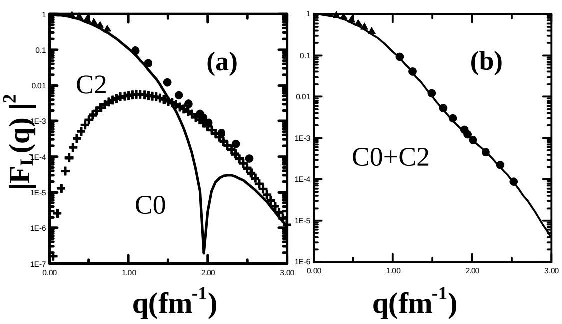


***Fig.(6) Same as caption to Fig.(4), but using*** $e_p$***=1.15e and*** $e_n$***=0.45e effective charges.The data are taken from Ref.[13] (circles) and Ref. [20] (triangles).***

## 4.Conclusion

The inclusion of the effects of effective charges effects modifies the form factors markedly and describes the experimental data very well in the momentum transfer dependence. Effective charges are essential in the calculation of C2 form factors. Effective charges calculations presented in the present work, succeeded in the describing the electron scattering data using the *p*-shell model space nuclei and at the *spsdpf*-shell model space.

The large no-core model space (model B) gives a good agreement with the model space A for all the region of momentum transfer ($q = 0 \rightarrow 3\,fm^{-1}$).

## References

[1] T.W. Donnelly, "Elastic magnetic electron scattering from nuclei", Rev. modern phys, Vol.**56, No.** 3-4, 1984, pp. 461-566.

[2] T. Sato, N. Odagana, H. Ohtsubo, and T. S.H. Lee, "Nuclear structure studies with $(e,e')$, $(p,p')$, and $(g,p)$ reactions application to $^{10}$B", Phys.Rev. **,** Vol. C94, 1994, pp. 776.

[3] D. Amit, and A. Katz, "Effective Interaction calculation of energy levels and wave function in the nuclear 1p-shell", Nucl. Phys., Vol.**58**, 1964, pp. 388-406.

[4] S.Cohen, D.Kurath, "Effective interactions for the 1p-shell", Nucl.Phys., Vol.73, 1965, pp. 1.

[5] D.C. Zheng, J.P Vary, B.R.Barrett, "Large-space shell-model calculations for light nuclei", Phys. Rev., Vol.C50, 1994, pp. 2841.

[6] D.C. Zheng, B.R.Barrett, J.P Vary, W.C.Haxton, C.-L.Song," Large-basis shell model studies of light nuclei with multivalued G-matrix effective interaction", Phys.Rev., Vol.C52**,** 1995, pp. 2488.

[7] P.Navratil, M.Thoresen, B.R. Barrett, "Microscopic origins of effective charges in the shell model", Phys.Rev., Vol.**C55,** 1997, pp. 573.

[8] S.Karataklidis, B.A.Brown, K.Amos, P.J.Dortmass, "Shell model structures of low-lying excited states in $^{6,7}$Li", Phys.Rev., Vol.C55**,** 1997, pp. 2826.

[9] P.Navratil, B.R. Barrett, W.E.Ormand, "Large –basis shell model calculation of the $^{10}C \rightarrow {}^{10}B$ Fermi matrix element", Phys.Rev, Vol.C56, 1997, pp. 2542.

[10] P.Navratil, B.R. Barrett,. "Large-basis shell-model calculations for p-shell nuclei", Phys. Rev., Vol.**C** 57**,** 1998, pp. 3119.

[11] R. A. Radhi, A. A. Abdullah, A. H. Raheem," Calculation of elastic and inelastic electron scattering on $^{19}F$ using large – basis no core – shell model wave functions", Nucl. Phys., Vol.A798, 2008, pp. 16-28.

[12] T.de Forest Jr., and J.D.Walecka, "Electron scattering and Nuclear structure", Adv.Phys., Vol.15**,** 1966, pp. 1.

[13] J.P.Glickman, W.Bertozzi, T.N.Buti, S.Dixit, F.W.Hersman, C.E.HydeWright, M.V.Hyns, R.W.Lourie and B.E.Norum, J.J.Kelly, B.L.Berman, D.J.Millener, "Electron scattering from $^{9}Be$", Phys.Rev., Vol.C43, 1991, pp. 2740.

[14] E.K.Warburton, B.A.Brown, "Effective interaction for the 0*p*1*s*0*d* nuclear shell-model space", Phys.Rev**.,** Vol.C46, 1992, pp. 923.

[15] E.K.Warburton, J.A.Becker, B.ABrown, Systematics for A=29-44 nuclei: "The de formed A~32 region", Phys.Rev., Vol.C41, 1990, pp. 1147.

[16] A.Hosaka, K.-I.Kubo, H.Toki, "G-matrix effective interaction wiyh the paris potential", Nucl. Phys., Vol. A444, 1985, pp. 76.

[17] B.A.Brown, B. H. Wildental," USD Hamiltonian for the sd shell", Annu. Rev. Nucl., Part.Sci. Vol.38, 1988, pp. 29.

[18] B.A.Brown, W.A.Richter, "New "USD" Hamiltonian for the sd", Phys. Rev**.,** Vol.C74, 2006, pp. 034315.

[19] B.A.Brown, A.Etchegoyen, N.S.Godwin, W.D.M.Rae, W.A.Richter, W.E.Ormand, E.K.Warburton, J.S.Winfield, L.Zhao, C.H.Zimmerman, "MSU-NSCL report number 1289 OXBASH pc computer code", version 2005.

[20] J.A.Jansen, R.Th.Peerdeman, and C.De Vries, "Nuclear charge radii of $^{12}C$ and $^{9}Be$", Nucl. Phys., Vol. A188, 1972, pp. 337-352.

[21] B.A.Brown, R.Radhi, B.H.Wildenthal, "Electric quadrupole and hexadecupole nuclear excitation from the perspectives of electron scattering and modren shell model theory", Phys. Rep., 101, 1983, pp. 313.



**الخلاصة**

تمت دراسة عوامل التشكل الطولية للأستطارة المرنة لنواة البريليوم $^{9}Be$ في المستوي (0.0MeV $J^{p} = 3/2^{-}, T = 1/2$) في اطار فضاء الأنموذج p- (shell model space) والمتمثل بالنويات الموزعة على مدارات القشرة (1p-shel l) خارج قلب النواة المتمثل بنواة الهيليوم $^{4}He$ حيث يتم توزيع خمسة نيوكليونات على القشرة ((1p-shell). واستخدم ايضا فضاء الانموذج بدون قلب No-core basis shell model with( **h***w* (0+2) لدراسة تأثير الشحنة الفعالة فتم حساب عوامل التشكل الطولية المرنة للحصول على نتائج متوافقة بصورة جيدة مع النتائج العملية في كلا الانموذجين وتم حساب شدة الانتقال المختزل B(C2) في كلا الانوذجين ولجيمع الشحنات الفعالة الستخدمة في موضوع البحث.